# Mollow Triplet under Incoherent Pumping

E. del Valle[1] and F. P. Laussy[2]

[1]School of Physics and Astronomy, University of Southampton, SO17 1BJ, Southampton, United Kingdom
[2]Walter Schottky Institut, Technische Universität München, Am Coulombwall 3, 85748 Garching, Germany

(Received 8 July 2010; published 1 December 2010)

A counterpart of the Mollow triplet (luminescence line shape of a two-level system under coherent excitation) is obtained for the case of incoherent excitation in a cavity. The system acquires coherence through the strong-coupling between the cavity and the emitter. Analytical expressions, in excellent agreement with numerical results, pinpoint analogies and differences between the conventional resonance fluorescence spectrum and its cavity QED analogue under incoherent excitation. Most notably, the satellites broaden and split sublinearly with increasing incoherent pumping.

DOI: 10.1103/PhysRevLett.105.233601 PACS numbers: 42.50.Pq, 42.50.Ct, 42.55.Sa, 78.47.N−

Mollow [1] discovered a striking type of spectral shape in the resonance fluorescence problem, where an atom is irradiated by a strong laser beam. The celebrated *Mollow triplet*, that results from transitions between atomic states that are dressed by the coherent light field, has since been a testbed of nonlinear optics. It stands as one of the fundamental spectral shapes of light-matter interaction, maybe second only to the Rabi doublet. Although the Mollow triplet is rooted in quantum physics and bears much quantum features itself, it arises from a fully classical light field. Its Hamiltonian, in the rotating frame of the laser and at resonance, simply reads $H_L = \Omega_L(\sigma + \sigma^\dagger)$, with $\Omega_L^2$ the laser intensity and $\sigma$ the only quantum operator, namely, the two-level system annihilation operator. Including the spontaneous decay of the emitter, in the Lindblad form $\mathcal{L}_\sigma(\rho) = (2\sigma\rho\sigma^\dagger - \sigma^\dagger\sigma\rho - \rho\sigma^\dagger\sigma)$, leads to a master equation $\partial_t\rho = i[\rho, H_L] + \frac{\gamma_\sigma}{2}\mathcal{L}_\sigma(\rho)$ from which one obtains the famous Mollow triplet line shape:

$$S_{\rm coh}(\omega) = \frac{\gamma_\sigma^2}{8\Omega_L^2 + \gamma_\sigma^2}\delta(\omega) + \frac{1}{2\pi}\frac{\frac{\gamma_\sigma}{2}}{(\frac{\gamma_\sigma}{2})^2 + \omega^2} + \frac{\gamma_\sigma}{\pi}\frac{16\Omega_L^2 - \gamma_\sigma^2 - \omega^2}{\gamma_\sigma^4 + 4(\omega^2 - 4\Omega_L^2)^2 + \gamma_\sigma^2(5\omega^2 + 16\Omega_L^2)}. \quad (1)$$

It is composed of an elastic scattering peak, the Dirac $\delta$ function, and the triplet itself, with a central Lorentzian peak of full width at half maximum (FWHM) $\gamma_\sigma$ and two satellite peaks at $\pm\Re(R_L)$ with Mollow splitting $R_L = \sqrt{(2\Omega_L)^2 - (\gamma_\sigma/4)^2}$ and FWHMs $3\gamma_\sigma/2$. This structure was observed a long time ago with atoms [2] and more recently also in a variety of solid state systems [3–7], with, as befits the above description, coherent excitation.

In this text we consider a close counterpart of this fundamental system, where the light field is initially fully quantized, and becomes continuous as a result of an incoherent and continuous pumping that feeds the system with a very large number of photons. This situation is realized—as for quantization of the light field—in cavity QED, where quanta of a trapped standing wave (the photons) interact with an isolated emitter, and—as for the incoherent pumping—with semiconductor microcavities [8], where excitations are continuously poured into the system with no external coherence fed in by a driving field. The role of the emitter is, in this case, played by a quantum dot placed in the antinode of the microcavity field. In the cavity QED version of the resonance fluorescence physics, the system is described by the Jaynes-Cummings Hamiltonian (still at resonance), $H = g(a^\dagger\sigma + a\sigma^\dagger)$, with the cavity mode also quantized through the boson operator $a$. Cavity and emitter decay $\gamma_{a/\sigma}$ and incoherent pumping $P_\sigma$ are described like before with a master equation:

$$\partial_t\rho = i[\rho, H] + \frac{\gamma_a}{2}\mathcal{L}_a(\rho) + \frac{\gamma_\sigma}{2}\mathcal{L}_\sigma(\rho) + \frac{P_\sigma}{2}\mathcal{L}_{\sigma^\dagger}(\rho), \quad (2)$$

where $\rho$ is now the density matrix for the combined two-level-emitter and cavity system. A transition from the Rabi doublet to a single lasing line was recently observed in the cavity emission when increasing pumping [9]. Since this has been claimed while remaining in strong-coupling, it results from climbing the Jaynes-Cummings ladder [10], and as such, is a successful realization of quantum nonlinearities in these systems. The importance of this breakthrough for microcavity-QED is however hindered by such a simple manifestation, particularly since other mechanisms can also result in a similar behavior of Rabi splitting collapse without entering the quantum nonlinear regime [11]. Here we propose another approach to evidence quantum features of the coupled quantum dot-microcavity system, by direct observation of the dot emission. This configuration is more difficult technically, especially in the star systems of photonic crystals, where side emission is mainly that of the cavity. Systems such as micropillars or microdisks might be more suited for observing the dot emission, by collecting photons from leaky modes, which can be done by measuring the light emitted in a perpendicular direction to that from the cavity axis. In general,

 

quantum features are better observed when probing the quantum emitter, rather than the cavity, whose close connections with the classical oscillator tend to surface rapidly and dominate strongly. Theoretical description is straightforward in the low excitation regime even when solving the system exactly [10], but it becomes computationally demanding when the lasing regime is approached. In this text, we consider the highly nonlinear regime of microcavity QED, that is, Jaynes-Cummings physics under a strong incoherent pumping. We find that, in good systems by the standard of today, a new type of Mollow triplet is obtained in the direct quantum dot emission spectrum. It is a close counterpart of the classical Mollow triplet where light is described by a classical field [1], whereas it is here described as numerous quanta of the cavity mode. The coherence is acquired through the strong-coupling with the dot, resulting in striking variations from the case where it is provided by an external laser. We now describe them analytically.

*Mollow regime.*—Whereas only one parameter (intensity) fully describes the light in Mollow's description, the Jaynes-Cummings picture requires from the start to take into account an infinite number of correlators between the fields, that we can however relate to each other [10]: $\langle a^{\dagger n} a^{n-1}\sigma\rangle = i\frac{\gamma_a}{2g}\langle a^{\dagger n}a^n\rangle$ and $\langle a^{\dagger n-1}a^{n-1}\sigma^\dagger\sigma\rangle = [P_\sigma\langle a^{\dagger n-1}a^{n-1}\rangle - \gamma_a\langle a^{\dagger n}a^n\rangle]/[\Gamma_\sigma + \gamma_a(n-1)]$ where we introduced $\Gamma_\sigma = \gamma_\sigma + P_\sigma$. From this follows a first relation for the populations of the modes, $n_\sigma = \langle\sigma^\dagger\sigma\rangle$ and $n_a = \langle a^\dagger a\rangle$, namely $n_\sigma = (P_\sigma - \gamma_a n_a)/\Gamma_\sigma$. This also allows us to obtain a self-contained equation for $\langle a^{\dagger n}a^n\rangle$:

$$\langle a^{\dagger n}a^n\rangle = \frac{\frac{nP_\sigma}{\Gamma_\sigma+(n-1)\gamma_a}\langle a^{\dagger n-1}a^{n-1}\rangle - \frac{2\gamma_a}{\Gamma_\sigma+n\gamma_a}\langle a^{\dagger n+1}a^{n+1}\rangle}{1 + \frac{\Gamma_\sigma+(2n-1)\gamma_a}{\kappa_\sigma} - \frac{2P_\sigma}{\Gamma_\sigma+n\gamma_a} + \frac{n\gamma_a}{\Gamma_\sigma+(n-1)\gamma_a}}, \tag{3}$$

where $\kappa_\sigma = 4g^2/\gamma_a$ is the Purcell rate of transfer of population from the dot to the cavity mode. This recurrence equation allows us to compute $\langle a^{\dagger n}a^n\rangle$ for all $n$ as a function of $n_a$ only. The solution for $n = 0$ gives a good approximation for the region where the cavity field behaves classically:

$$n_a \approx \frac{\Gamma_\sigma}{2\gamma_a}\left(1 - \frac{\Gamma_\sigma - \gamma_a}{\kappa_\sigma} - \frac{2\gamma_\sigma}{\Gamma_\sigma}\right) \quad \text{and}$$
$$n_\sigma \approx \frac{1}{2}\left(1 + \frac{\Gamma_\sigma - \gamma_a}{\kappa_\sigma}\right). \tag{4}$$

The quality of this approximation is seen in Fig. 1 where it is compared with the exact solution, computed numerically [10]. The second order coherence function $g^{(2)}$ also admits a closedform expression (not given here but plotted in Fig. 1) which is unity in good approximation. The expressions Eqs. (4) for the populations have a clear physical meaning: at low pump, but still high enough to be beyond the quantum regime [10], i.e., $\gamma_\sigma,\ \gamma_a < P_\sigma \ll \kappa_\sigma$, the cavity population increases linearly with pumping, with a half occupied dot. This is the most effective region for accumulation of photons in the cavity (the so-called *one-atom laser* [12]), with little disruption from incoherent processes. Although less efficiently, the dot occupation also increases linearly with pumping, eventually quenching the linear increase of the cavity population. These expressions are thus valid until the dot population is fully inverted, at $P_{\max} \approx \kappa_\sigma$, then the self-quenching dominates the dynamics, emptying the cavity that goes to a thermal state. The maximum population of the cavity, $\max(n_a) \approx g^2/(2\gamma_a^2)$, is reached at the intermediate rate $P_\sigma \approx \kappa_\sigma/2$. This identifies the regime of interest for the observation of the Mollow triplet, where the cavity field is intense ($n_a \gg 1$) and coherent (with a Poissonian photon distribution, $T[n] = e^{-n_a}n_a^n/n!$ and $g^{(2)} = 1$):

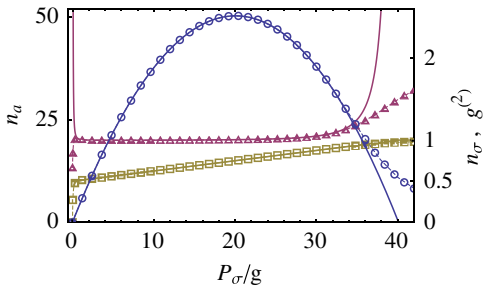


FIG. 1 (color online). Exact numerical solution (points) and their analytical approximation, Eqs. (4) (lines), for $n_a$ (blue, circles), $n_\sigma$ (brown, squares) and $g^{(2)}$ (pink, triangles), for $\gamma_a = 0.1g$ and $\gamma_\sigma = 0$, as a function of pumping $P_\sigma/g$. Analytical solutions become unphysical when $P_\sigma = \kappa_\sigma$ (here at $40g$), where $n_a = 0$, $n_\sigma = 1$ and $g^{(2)}$ diverges. They are very good approximations in the region of interest, Eq. (5).

$$\gamma_\sigma,\ \gamma_a \ll g < P_\sigma < \kappa_\sigma. \tag{5}$$

Now that we have a good and analytical description of the populations, we turn to the optical emission spectrum, that we show can be obtained in equally good approximations. The dot emission reads $n_\sigma\pi S_{\text{inc}}(\omega) \equiv \Re\int_0^\infty\langle\sigma^\dagger(0)\sigma(\tau)\rangle e^{i\omega\tau}d\tau$. We compute the two-time correlator $\langle\sigma^\dagger(0)\sigma(\tau)\rangle$ in two steps: first, we solve the master equation in the steady state, finding the density matrix elements $\rho_{m,i;n,j}$ (for $m,\ n \in \mathbf{N}$ and $i,\ j \in \{0, 1\}$, photon and exciton indexes, respectively). For the range of parameters of interest, we show that they can be analytically expressed in terms of the photon distribution $T[n]$ only. Second, we apply the quantum regression formula.

*1. Steady state density matrix.*—We consider only elements that are nonzero in the steady state: the populations $p_i[n] = \rho_{n,i;n,i}$ with $i = 0, 1$, corresponding to the probability to have $n$ photons with ($p_1$) or without ($p_0$) exciton, and the off-diagonal terms $q_i[n] = \Im(\rho_{n,0;n-1,1})$, corresponding to the coherence between the states $|n, 0\rangle$ and $|n-1, 1\rangle$. The master equation now reads

$$\partial_t p_0[n+1] = \mathcal{D}_{\text{phot}}\{p_0[n+1]\} + \gamma_\sigma T[n+1] - \Gamma_\sigma p_0[n+1] - 2g\sqrt{n+1}\,q_i[n+1], \quad (6a)$$

$$\partial_t p_1[n] = \mathcal{D}_{\text{phot}}\{p_1[n]\} + P_\sigma T[n] - \Gamma_\sigma p_1[n] + 2g\sqrt{n+1}\,q_i[n+1], \quad (6b)$$

$$\partial_t q_i[n+1] = \mathcal{D}_{\text{phot}}\{q_i[n+1]\} - \frac{\Gamma_\sigma}{2} q_i[n+1] + g\sqrt{n+1}(p_0[n+1] - p_1[n]), \quad (6c)$$

where we have separated the photonic dynamics into a superoperator $\mathcal{D}_{\text{phot}}$. Given that it is much slower than the dot dynamics, one can solve the steady state ignoring $\mathcal{D}_{\text{phot}}$ [13]. The photon distribution, $T[n] = p_0[n] + p_1[n]$, remains unperturbed during the excitation and interaction with the dot and Eqs. (6) then admit exact solutions in terms of $T[n]$.

*2. Two-time correlator and spectra.*—The two-time correlator can be expressed as a sum $\langle\sigma^\dagger(0)\sigma(\tau)\rangle = \sum_{n=0}^{\infty} Q[n](\tau)$, where $Q[n]$ and other functions $S_{0,1}[n]$ and $V[n]$ are defined through the quantum regression formula by coupled differential equations ($n \geq 0$):

$$\partial_\tau Q[n] = \mathcal{D}_{\text{phot}}\{Q[n]\} - \frac{\Gamma_\sigma}{2} Q[n] + ig(\sqrt{n}S_1[n] - \sqrt{n+1}S_0[n+1]), \quad (7a)$$

$$\partial_\tau S_0[n+1] = \mathcal{D}_{\text{phot}}\{S_0[n+1]\} + \gamma_\sigma X[n+1] - \Gamma_\sigma S_0[n+1] + ig(\sqrt{n}V[n+1] - \sqrt{n+1}Q[n]), \quad (7b)$$

$$\partial_\tau S_1[n] = \mathcal{D}_{\text{phot}}\{S_1[n]\} + P_\sigma X[n] - \Gamma_\sigma S_1[n] - ig(\sqrt{n+1}V[n+1] - \sqrt{n}Q[n]), \quad (7c)$$

$$\partial_\tau V[n+1] = \mathcal{D}_{\text{phot}}\{V[n+1]\} - \frac{\Gamma_\sigma}{2} V[n+1] + ig(\sqrt{n}S_0[n+1] - \sqrt{n+1}S_1[n]). \quad (7d)$$

They are, like for the single-time dynamics, separated into a slow photonic dynamics embedded in a superoperator $\mathcal{D}_{\text{phot}}$ that is $\tau$ independent in good approximation, and a fast exciton and coupling dynamics that we can solve analytically. Moreover, we have introduced the steady state function $X[n] \equiv S_0[n](0) + S_1[n](0)$, in analogy with $T[n]$. The initial conditions in Eq. (7) are the steady state values $S_0[n+1](0) = iq_i[n+1]$, $S_1[n](0) = 0$, $Q[n](0) = p_1[n]$ and $V[n+1](0) = 0$ (therefore, $X[n] = iq_i[n]$). After some long, but straightforward algebra, we can find the expression for $Q[n](\tau)$ in terms of $p_{0,1}[n]$ and $q_i[n]$, which, in turn, are expressed in terms of the statistics $T[n]$. This allows us to compute a closed-form solution for $\langle\sigma^\dagger(0)\sigma(\tau)\rangle$, which is however lengthy and not worth writing here. It shows that each term in the sum over $n$ accounts for the four transitions between adjacent rungs $n+1$ and $n$ [10]. The linear regime ($n = 0$) consists of only the two transitions of the Rabi doublet. Other rungs give rise to a generalization of the Rabi frequency in the nonlinear regime: the *nth-rung inner* and *outer Rabi frequencies*, $R_{O,I}[n] = \sqrt{g^2(\sqrt{n+1} \pm \sqrt{n})^2 - (\Gamma_\sigma/4)^2}$. In the Mollow triplet regime ($P_\sigma > g$), all the peaks positioned at the inner frequencies collapse at the center (including the Rabi doublet) giving rise to a single central peak. Outer peaks remain split at frequencies $\pm R_O[n] \approx \pm\sqrt{4g^2 n - (\Gamma_\sigma/4)^2}$.

The spectrum just obtained can be further simplified for the range of parameters in Eq. (5), to give a compact analytical expression. First, one considers only the coefficients with leading terms in $n$, making use of $n+1 \approx n$. Then, due to the Poissonian statistics, only rungs with $n$ close to $n_a$ contribute significantly allowing the substitution $n \to n_a$ in $Q[n]$. The sum over $n$ simplifies thanks to the normalization of the distribution function: $\sum_n T[n] = 1$. Finally, we neglect terms related to $\gamma_a$ before those related to much larger rates, $P_\sigma$ and $\kappa_\sigma$, i.e., we write the spectrum for these three rates only, through the substitution $g^2 = \kappa_\sigma\gamma_a/4$, and set $\gamma_a \to 0$. This results in the expression for $S_{\text{inc}}(\omega)$ in terms of $P_\sigma$, $\gamma_\sigma$ and $\kappa_\sigma$ only, with $C_\delta = \left(\frac{2P_\sigma}{\kappa_\sigma+\Gamma_\sigma} - \frac{\Gamma_\sigma}{\kappa_\sigma}\right)$:

$$S_{\text{inc}}(\omega) = C_\delta\delta(\omega) + \frac{\frac{1}{2\pi}\frac{\Gamma_\sigma}{2}}{(\frac{\Gamma_\sigma}{2})^2 + \omega^2} + \frac{(P_\sigma - \gamma_\sigma)(3\Gamma_\sigma^3 - (P_\sigma - 5\gamma_\sigma)\Gamma_\sigma\kappa_\sigma + 2\gamma_\sigma\kappa_\sigma^2) - (\Gamma_\sigma^2 - (3P_\sigma - \gamma_\sigma)\kappa_\sigma)\omega^2}{\pi(\kappa_\sigma + \Gamma_\sigma)(9\Gamma_\sigma^2\omega^2 + [2\omega^2 - \kappa_\sigma(P_\sigma - \gamma_\sigma)]^2)}. \quad (8)$$

This is our main result. The structure of the line shape is the same as that of its coherent counterpart, Eq. (1): a Dirac $\delta$ function from the elastically scattered laser light superimposed to a triplet. The central Lorentzian peak has the same weight 1/2 but with FWHM given by the decoherence rate $\Gamma_\sigma$. The two satellite peaks sit at $\pm\Re(R_O)$ with Mollow splitting

$$R_O = \sqrt{(P_\sigma - \gamma_\sigma)\kappa_\sigma/2 - (3\Gamma_\sigma/4)^2} \quad (9)$$

and FWHM $3\Gamma_\sigma/2$. The excellent agreement of our formula with exact numerical results [10,14] is shown in Fig. 2(a), where we superimpose in dashed blue the numerical computation to, in solid red, the analytical expression Eq. (8). Note the elastic peak in the numerics as a very narrow central line.

Despite a similar structure, the line shapes of Eqs. (1) and (8) are intrinsically different. This can be appreciated on physical grounds, when the laser intensity for the

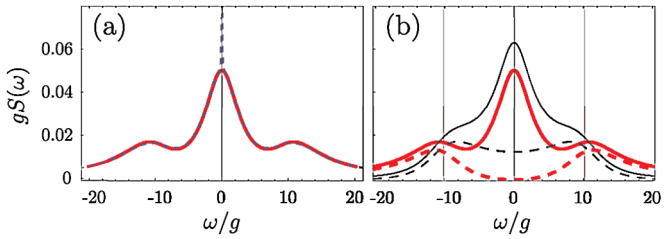


FIG. 2 (color online). (a) Comparison between analytical expression Eq. (8), without the elastic peak, (solid red) and the exact numerical solution (dashed blue). (b) Difference between the incoherent (thick solid, red line) and the coherent (thin solid, black line) Mollow triplets, in equivalent conditions. The satellite peaks, that cause the departure, are plotted in dashed. Parameters: $P_\sigma = 6.3g$, $\gamma_a = 0.1g$ and $\gamma_\sigma \to 0$.

conventional Mollow triplet is taken the same as the average population of the cavity under incoherent excitation (i.e., $\Omega_L^2 \to g^2 n_a$), and when the broadening of the dot includes $P_\sigma$ (i.e., $\gamma_\sigma \to \Gamma_\sigma$). In this way, we attempt the description of the incoherent system with the theory of the coherent one. We obtain an expression that shows the fundamental discrepancies between the two types of triplets:

$$S'_{\mathrm{coh}}(\omega) = \frac{\Gamma_\sigma^2}{\kappa_\sigma(P_\sigma - \gamma_\sigma)}\delta(\omega) + \frac{\frac{1}{2\pi}\frac{\Gamma_\sigma}{2}}{(\frac{\Gamma_\sigma}{2})^2 + \omega^2} - \frac{1}{\pi}\frac{\Gamma_\sigma(3\Gamma_\sigma^2 - 2\kappa_\sigma(P_\sigma - \gamma_\sigma) + \omega^2)}{9\Gamma_\sigma^2\omega^2 + [2\omega^2 - \kappa_\sigma(P_\sigma - \gamma_\sigma)]^2}. \quad (10)$$

Comparing this expression with Eq. (8), the central peak is the same in both cases, as well as the position and broadening of the satellite peaks (third terms have the same denominator), so the underlying structures bear some similarities. However, the satellite line shapes differ, being affected by the effect of incoherent pumping and factors such as the dot population, which under coherent excitation shows opposite behavior to that of Eq. (4): $n'_{\sigma,\mathrm{coh}} \approx \frac{1}{2}[1 - \Gamma_\sigma^2/(\kappa_\sigma(P_\sigma - \gamma_\sigma))]$. The shapes of these peaks are shown in Fig. 2(b), where they are plotted (in dashed) together with the whole triplets, in the coherent (thin black) and the incoherent (thick red) cases.

Finally, Fig. 3 shows the natural experimental configuration to demonstrate the new character of nonlinear spectroscopy in microcavities under incoherent pumping, and to contrast it with its coherent counterpart. Increasing pumping, one sees that in the coherent case (upper panel), the triplet is better resolved, with a larger splitting, while in the incoherent case (lower panel), the satellites overlap with the central line as a result from pumping that splits them sublinearly, Eq. (9), and also increases their broadening. The two phenomenologies, despite their deep interconnections and common features, are strikingly different and the evidence of the new one should pose no problem even on qualitative grounds. Observation of the Mollow triplet under incoherent pumping would inaugurate a new era bringing together quantum coherence and nonlinearities in microcavities, shedding light on coherence buildup, lasing and strong coupling.

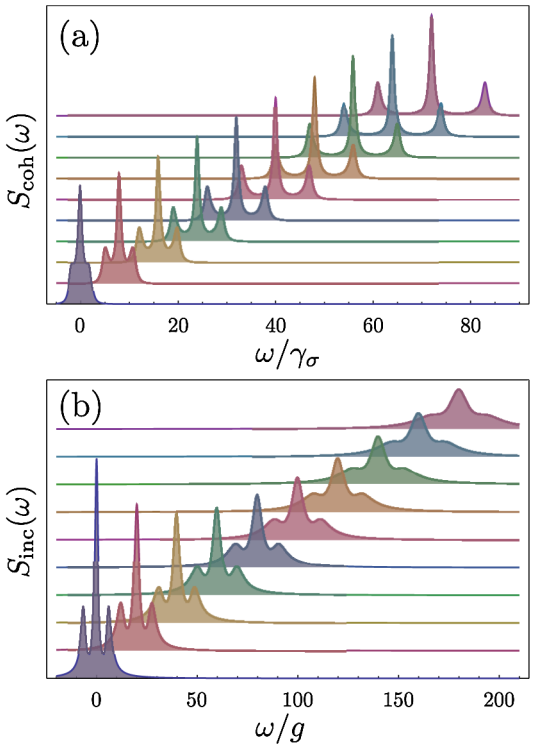


FIG. 3 (color online). Evolution of the Mollow triplet when increasing (from bottom to top) (a) coherent ($\Omega_L/\gamma_\sigma$ from 1 to 5.5 by steps of 0.5) and (b) incoherent ($P_\sigma/g$ from 2 to 11 by steps of 1, for $\gamma_a = 0.1g$ and $\gamma_\sigma \to 0$) excitation.

We acknowledge support of a Newton International Fellowship and FP7-PEOPLE-2009-IEF project 'SQOD.'

[1] B. R. Mollow, Phys. Rev. **188**, 1969 (1969).
[2] F. Y. Wu, R. E. Grove, and S. Ezekiel, Phys. Rev. Lett. **35**, 1426 (1975).
[3] A. Muller *et al.*, Phys. Rev. Lett. **99**, 187402 (2007).
[4] S. Ates *et al.*, Phys. Rev. Lett. **103**, 167402 (2009).
[5] E. B. Flagg *et al.*, Nature Phys. **5**, 203 (2009).
[6] A. N. Vamivakas, Y. Zhao, C.-Y. Lu, and M. Atatüre, Nature Phys. **5**, 198 (2009).
[7] O. Astafiev *et al.*, Science **327**, 840 (2010).
[8] E. del Valle, *Microcavity Quantum Electrodynamics* (VDM Verlag, Saarbrücken, Germany, 2010).
[9] M. Nomura, N. Kumagai, S. Iwamoto, Y. Ota, and Y. Arakawa, Nature Phys. **6**, 279 (2010).
[10] E. del Valle, F. P. Laussy, and C. Tejedor, Phys. Rev. B **79**, 235326 (2009).
[11] S. Münch *et al.*, Opt. Express **17**, 12821 (2009).
[12] Y. Mu and C. M. Savage, Phys. Rev. A **46**, 5944 (1992).
[13] M. O. Scully and M. S. Zubairy, *Quantum Optics* (Cambridge University Press, Cambridge, England, 2002).
[14] M. Löffler, G. M. Meyer, and H. Walther, Phys. Rev. A **55**, 3923 (1997).